

# Retrieval of tropospheric column densities of NO<sub>2</sub> from combined SCIAMACHY nadir/limb measurements

S. Beirle, S. Köhl, J. Pukite, and T. Wagner

Max-Planck-Institut für Chemie, Mainz, Germany

Received: 6 November 2009 – Published in Atmos. Meas. Tech. Discuss.: 23 November 2009

Revised: 16 February 2010 – Accepted: 23 February 2010 – Published: 25 February 2010

**Abstract.** The SCIAMACHY instrument onboard the ESA satellite ENVISAT allows measurements of various atmospheric trace gases, such as NO<sub>2</sub>. A unique feature of SCIAMACHY is that measurements are made alternately in limb and nadir mode. The limb measurements provide an opportunity for directly determining stratospheric column densities (CDs), which are needed to extract tropospheric CDs from the total CD measurements performed in (quasi simultaneous) nadir geometry.

Here we discuss the potential and limitations of SCIAMACHY limb measurements for estimating stratospheric CDs of NO<sub>2</sub> in comparison to a simple reference sector method, and the consequences for the resulting tropospheric CDs. A direct, absolute limb correction scheme is presented that improves spatial patterns of tropospheric NO<sub>2</sub> column densities at high latitudes, but results in artificial zonal stripes at low latitudes. Subsequently, a *relative* limb correction scheme is introduced that successfully reduces stratospheric artefacts in the tropospheric data product without introducing new ones. This relative limb correction scheme is rather simple, robust, and, in essence, based on measurements alone.

The effects of the different stratospheric estimation schemes on tropospheric CDs are discussed with respect to zonal and temporal dependencies. In addition, we define error quantities from the nadir/limb measurements that indicate remaining systematic errors as a function of latitude and day.

Our new suggested stratospheric estimation scheme, the relative limb correction, improves mean tropospheric slant CDs significantly, e.g. from  $-1 \times 10^{15}$  molec/cm<sup>2</sup> (using a reference sector method) to  $\approx 0$  in the Atlantic ocean, and from  $+1 \times 10^{15}$  molec/cm<sup>2</sup> to  $\approx 0$  over Siberia, at 50° N in January 2003–2008.

## 1 Introduction

Satellite-borne UV-vis spectrometers, like the Global Ozone Monitoring Experiment (GOME 1 & 2), the Scanning Imaging Absorption spectrometer for Atmospheric CHartography (SCIAMACHY), or the Ozone Monitoring Instrument (OMI) (e.g. Burrows et al., 1999; Bovensmann et al., 1999; Levelt et al., 2006), originally designed for monitoring stratospheric ozone, are also used for the retrieval of other atmospheric trace gases like NO<sub>2</sub>, SO<sub>2</sub>, H<sub>2</sub>O, OClO, BrO, IO, HCHO, or CHOCHO, on global scale (e.g. Burrows et al., 1999; Martin et al., 2008; Wagner et al., 2008). In particular the retrieval of tropospheric NO<sub>2</sub> column densities has been demonstrated and analyzed in several studies with numerous scientific applications in recent years (see for instance Martin et al., 2008, and references therein).

From the spectrally resolved nadir measurements, total slant column densities (SCDs), i.e. concentrations integrated along the effective light path, are derived by differential optical absorption spectroscopy (DOAS) (Platt and Stutz, 2008) or similar techniques. SCDs can be transformed to vertical column densities (VCDs) by accounting for radiative transfer in the atmosphere. Note that in the following we use the inspecific term “column densities” (CDs), but define and discuss the matter of vertical versus slant column densities in detail in Sects. 2.4 and 2.5.

If one is interested in tropospheric CDs of trace gases that are present both in stratosphere and troposphere, the stratospheric fraction has to be removed from the total atmospheric CDs. This is a particularly challenging task in the case of O<sub>3</sub>, since the bulk of the total CD is located in the stratosphere. Different methods are in use to estimate stratospheric ozone CDs e.g. from nadir measurements over clouded scenes (“cloud slicing”, Ziemke et al., 2001), or from additional measurements in limb or occultation geometry like SAGE (Fishman and Balok, 1999).



Correspondence to: S. Beirle  
(steffen.beirle@mpic.de)

In this study, we focus on stratospheric estimation schemes (SES) for NO<sub>2</sub>. The choice of the SES has significant impact on the retrieved tropospheric CDs of NO<sub>2</sub> and leads to systematic differences between retrieval schemes. Generally, there are three approaches for the estimation of stratospheric CDs, using (1) atmospheric chemistry models, (2) a subset of the satellite measurements which are assumed to be free of tropospheric pollution, and (3) additional (more or less) direct measurements of the stratospheric CD.

(1) Atmospheric chemistry models directly provide information on stratospheric CDs which can be used for the retrieval of tropospheric CDs. Richter et al. (2005) take stratospheric CDs of NO<sub>2</sub> from the SLIMCAT model for their stratospheric estimation. Boersma et al. (2007) use a data assimilation approach with the TM4 model.

While stratospheric NO<sub>x</sub> chemistry is in general understood quite well, the utilization of chemistry models for the stratospheric estimation nevertheless has its drawbacks. First, models and measurements are generally not in perfect agreement, but have systematic biases dependent on time, latitude, and/or observation geometry. Hence, model CDs have to be “tuned” – somewhat arbitrarily – to match observations (see Richter et al., 2005). Second, in the case of data assimilation, a-priori knowledge on the global tropospheric NO<sub>2</sub> distribution is needed; in case of a (faulty) stratospheric classification of a signal of tropospheric origin, it would be assimilated in the stratosphere. Third, the resulting tropospheric CDs are not independent measurements any more.

(2) In several stratospheric correction schemes the satellite measurements themselves are used to define subsets of data that are assumed to represent the stratospheric CD. These subsets are inter- or extrapolated to global fields afterwards.

A quite simple stratospheric correction scheme for NO<sub>2</sub> is the reference sector method (RSM) (e.g. Richter and Burrows, 2002; Martin et al., 2002; Beirle et al., 2003): The stratospheric CD at a given latitude is estimated from measurements over the remote Pacific (at the respective latitude), which can be considered to be unpolluted. Note that this approach is only applicable for satellites operated in sun-synchronous orbit, so that the *local* time of measurements in and outside the reference sector is the same. The RSM generally results in tropospheric *excess* CDs w.r.t. the reference sector. Within the RSM approach, longitudinal variations of stratospheric NO<sub>2</sub> are neglected, which generally works well for low and mid-latitudes, but may fail especially at higher latitudes, in particular close to the polar vortices (e.g. Richter and Burrows, 2002; Martin et al., 2002; Boersma et al., 2004; Sierk et al., 2006).

Some refinements of the simple RSM have been discussed, which take longitudinal variations of stratospheric CDs into account, but still estimate them from the measurements alone. Leue et al. (2001) and Wenig et al. (2004) define unpolluted reference regions around the globe (instead of just one band in the Pacific) and interpolate the stratospheric 2-FD field. Bucselá et al. (2006) perform a Wave-2

fitting along zonal bands. While these refined RSM methods account for longitudinal variations, they require the (rather arbitrary) selection of “unpolluted” regions which must neither be too small (which could lead to interpolation errors and possibly to overshoots of the interpolated stratosphere over the large “polluted” area) nor too large (which could lead to the false classification of a smooth continental tropospheric background in the “unpolluted” region, e.g. from soil emissions, as stratospheric NO<sub>2</sub>). These difficulties are amplified in the case of SCIAMACHY due to its poor spatial coverage (compared to GOME/GOME-2 or OMI).

(3) SCIAMACHY is the first satellite instrument that combines limb and nadir measurements. The viewing geometry alternates between nadir and limb states in such a way, that the atmosphere is first scanned in limb (allowing the retrieval of stratospheric profiles), and subsequently in nadir geometry (providing total CDs for approximately the same air mass) (see Bovensmann et al., 1999). This “Limb-Nadir-Matching” was intended to provide direct measurements of stratospheric CDs corresponding to the successive nadir CD measurements.

For NO<sub>2</sub> and O<sub>3</sub>, the potential of SCIAMACHY limb measurements for stratospheric correction has already been demonstrated exemplarily (Sioris et al., 2004; PROMOTE, 2004; Sierk et al., 2006; Heckel et al., 2007). However, to the authors’ knowledge, no standard data product of tropospheric NO<sub>2</sub> is currently retrieved utilizing limb data for stratospheric correction.

Here we discuss the potential of limb measurements for stratospheric correction of total NO<sub>2</sub> CDs. We compare the simple RSM to a direct, absolute limb correction (ALC), which improves spatial patterns of tropospheric CDs, in particular over and around the polar vortex, but introduces artefacts elsewhere. We also present a *relative* limb correction scheme (RLC), where the limb data is “corrected” for the reference sector (RS), analogue to the nadir RSM, and just the *longitudinal variations* of the limb data are used to improve the stratospheric estimation from the simple RSM. This relative limb correction scheme is simple and robust with respect to possible biases in nadir and/or limb retrievals and their potential dependency on location and time, as long as these biases affect CDs in and out of the RS alike. It is, in essence, free of model input, but based on the satellite measurements.

The RLC scheme is a significant improvement over the simple RSM, yielding more plausible tropospheric NO<sub>2</sub> CDs. In particular over the Northern Atlantic in winter, where the RSM results in large negative tropospheric CDs, the RLC yields realistic tropospheric CDs close to zero. RLC modifications for lower latitudes are less pronounced (compare e.g. Richter and Burrows, 2002; Martin et al., 2002; Boersma et al., 2004), but still significant over large parts of the continents, even over regions of strong NO<sub>x</sub> emissions, like Europe or the east coast of the United States. Thus, the choice of the SES has a significant impact on quantitative

studies (like emission estimates) based on NO<sub>2</sub> CDs from satellite measurements.

## 2 Data and methods

In this section we shortly describe the characteristics of the SCIAMACHY instrument (Sect. 2.1) and our retrieval schemes of NO<sub>2</sub> nadir CDs (Sect. 2.2) and limb profiles (Sect. 2.3).

We discuss different stratospheric estimation schemes (SES) in Sect. 2.4: first (Sect. 2.4.1) the simple reference sector method (RSM), second (Sect. 2.4.2), an absolute limb correction (ALC) scheme, and third (Sect. 2.4.3), a relative limb correction (RLC) scheme. From these three stratospheric estimation schemes, we accordingly derive three tropospheric products (Sect. 2.5), which are compared and discussed in Sects. 3 (results) and 4 (discussion).

In Sect. 2.6 we discuss to which extent information on statistical as well as systematic errors of tropospheric CDs can be gained from the limb/nadir measurements themselves.

The different SES are illustrated exemplarily for 28 January 2006. Additional examples for other times of the year, as well as a more in-depth discussion of error quantities, are presented in a supplementary document, referred to as “Supplement” hereafter (see <http://www.atmos-meas-tech.net/3/283/2010/amt-3-283-2010-supplement.pdf>).

Table 1 gives an overview on the symbols and abbreviations used in this study.

### 2.1 SCIAMACHY

The Scanning Imaging Absorption spectrometer for Atmospheric CHartography, SCIAMACHY (Bovensmann et al., 1999), was launched onboard the ESA satellite ENVISAT in March 2002. ENVISAT orbits the Earth in a sun-synchronous orbit with an inclination from the equatorial plane of 98.5°. It performs one orbit in approx. 100 min, with a local equator crossing time of about 10:00 a.m. in descending node.

SCIAMACHY measures Earthshine spectra from the UV to the NIR with a spectral resolution of 0.22–1.48 nm. It is operated in different viewing geometries, including nadir, limb, and solar/lunar occultation. In nadir geometry (i.e. directed vertically, perpendicular to the Earth’s surface), the instrument performs an across-track scan of about ±32°, equivalent to a swath-width of 960 km. The footprint of a single nadir observation is typically 30 × 60 km<sup>2</sup>. Global cover of nadir measurements is achieved after 6 days. In limb geometry (i.e. directed horizontally, tangential to the Earth’s surface), the instrument performs scans in flight direction with elevation steps of approx. 3.3 km at the tangent point. The cross-track swath is 960 km, as for the nadir measurements, and consists of up to 4 pixels. The field of view at the

tangent point is about 2.5 km (vertically) × 110 km (horizontally). The limb scanning allows the retrieval of stratospheric profiles of NO<sub>2</sub> (see Sect. 2.3).

In standard operation, the measurement state alternates between limb and nadir in such a way that the limb measurements probe (almost) the same stratospheric air mass as the subsequent nadir measurements. Note that the term “state” in the following is used to denote the SCIAMACHY measurement mode as well as to summarize the entity of measurements performed within one nadir/limb state.

### 2.2 Retrieval of total slant column densities of NO<sub>2</sub>: nadir

Slant column densities (SCDs)  $S$  of NO<sub>2</sub> are derived from SCIAMACHY nadir spectra using Differential Optical Absorption Spectroscopy DOAS (Platt and Stutz, 2008). Cross-sections of O<sub>3</sub>, NO<sub>2</sub>, O<sub>4</sub>, H<sub>2</sub>O and CHOCHO are fitted in the spectral range 430.8–459.5 nm. In addition, Ring spectra, accounting for inelastic scattering in the atmosphere (rotational Raman) as well as in liquid water (vibrational Raman), an absorption cross-section of liquid water, and a polynomial of degree 5 are included in the fit procedure. A daily solar measurement is used as Fraunhofer reference spectrum.

This NO<sub>2</sub> DOAS retrieval setup is different from previous versions (e.g. Beirle, 2004) in so far that liquid water absorption and vibrational Raman scattering on liquid water molecules, which have been shown to affect spectra in the UV/vis (Vasilkov et al., 2002; Vountas et al., 2007), is now accounted for. This modification improves the spectral fits over oligotrophic oceanic regions (Polovina et al., 2008), where NO<sub>2</sub> SCDs of the previous fit version show a systematic negative bias. The remaining (but significantly smaller) systematic spatial patterns over oligotrophic oceanic regions are subject to further investigations. These effects are related to this study in that large parts of the chosen reference region in the Pacific cover oligotrophic regions. With the current settings, the remaining biases over oceans are rather small (see discussion). Information on statistical and possible systematic fit errors can be derived from the standard deviation of NO<sub>2</sub> CDs in the reference sector (RS) (see Sect. 2.6).

In the DOAS set-up, a single NO<sub>2</sub> cross-section for a temperature of 220 K is included (Vandaele et al., 1998), which is appropriate for the stratosphere. Tropospheric CDs have to be corrected by a factor of about 1.2, to account for the temperature dependency of the NO<sub>2</sub> cross-section (see Boersma et al., 2004).

For this study, we only consider measurements from the descending part of the orbit with solar zenith angles (SZA) < 80°, since for higher SZA, the sensitivity for the troposphere becomes rather small. No cloud filter is applied, because in this study, our aim is an improved stratospheric estimation scheme, and the impact of clouds on stratospheric CDs is negligible.

**Table 1.** Abbreviations and Variables used in this study.

Symbol	Abbreviation	Quantity
	SZA	Solar Zenith Angle
	LZA	Line of sight Zenith Angle
$\Lambda$	lat	latitude
$\Phi$	lon	longitude
$d$		day (time variable)
	CD	Column Density
$S$	SCD	Slant Column Density
$V$	VCD	Vertical Column Density
$V^*$		VCD derived with stratospheric AMF
$W$		Stratospheric VCD
$A$	AMF	Air Mass Factor
$L$	LVCD	Limb Vertical Column Density (integrated profile)
$T$	TSCD	Tropospheric Slant Column Density
subscript <sub>RS</sub>	RS	(in the) Reference Sector
subscript <sub>Strat</sub>		Stratospheric
	SES	Stratospheric Estimation Scheme
	RSM	SES 1: Reference Sector Method
	ALC	SES 2: Absolute Limb Correction
	RLC	SES 3: Relative Limb Correction
$\Delta L$	LLV	Longitudinal Limb Variation
$s$	std	Standard deviation
$\delta$		Error
$\hat{\phantom{L}}$	LUT	Smoothed and interpolated look up table
	NH	Northern Hemisphere
	SH	Southern Hemisphere

### 2.3 Retrieval of stratospheric NO<sub>2</sub> profiles: limb

An algorithm for the retrieval of NO<sub>2</sub>, BrO and OClO vertical profiles from SCIAMACHY limb measurements was developed in our group (Puķīte et al., 2006; Kühn et al., 2008). The retrieval is performed in two steps: In the first step, SCDs are derived from the SCIAMACHY limb spectra at different tangent heights by DOAS. For NO<sub>2</sub> the fit-window ranges from 420 to 450 nm. The NO<sub>2</sub> cross-section at 223 K is taken from Bogumil et al. (2003). As reference spectrum we use a measurement at a tangent height where the absorption of the considered trace gas is small, i.e. for NO<sub>2</sub> at  $\sim 42$  km.

Second, the trace gas SCDs are converted into a vertical concentration profile by an inversion scheme based on a least squares approach (see e.g. Menke, 1999). To increase the signal-to-noise ratio, only one averaged SCD per tangent height is applied for the inversion (i.e. the SCD results of the four measured spectra per tangent height are co-added).

For the inversion, box air mass factors (AMFs) are calculated with the 3-D fully spherical Monte Carlo radiative transfer model (RTM) “McArtim” (Deutschmann, 2009), using temperature, pressure and ozone data from a model simulation provided by Brühl and Crutzen (1993). It should be noted that in some individual cases the actual temperature, pressure and ozone profile might differ considerably from the

assumed model profiles. No aerosols and clouds are assumed for the calculation of the box AMFs. The aerosol extinction is much lower compared to extinction by Rayleigh scattering in the stratosphere. Also, due to the limb viewing geometry and the narrow field of view, SCDs derived from measured spectra are practically insensitive to the atmosphere below the tangent height.

From sensitivity studies it was found that the related errors in the profile retrieval are on the order of a few percent in the upper and middle stratosphere (i.e. where the peak of NO<sub>2</sub> occurs) but can be up to 30% for altitudes around 15 km.

In comparison studies a good agreement of the retrieved BrO and NO<sub>2</sub> profiles with correlated balloon validation measurements was found (Dorf et al., 2006; Butz et al., 2006; Kühn et al., 2008; Puķīte et al., 2009). NO<sub>2</sub> profiles were compared for mid and high latitudes for autumn and spring and showed a good agreement regarding the shape of the profile, the altitude of the peak, and the absolute values, with discrepancies of within 5–15% for altitudes around the peak.

For the algorithm details please refer to Puķīte et al. (2006) and Kühn et al. (2008).

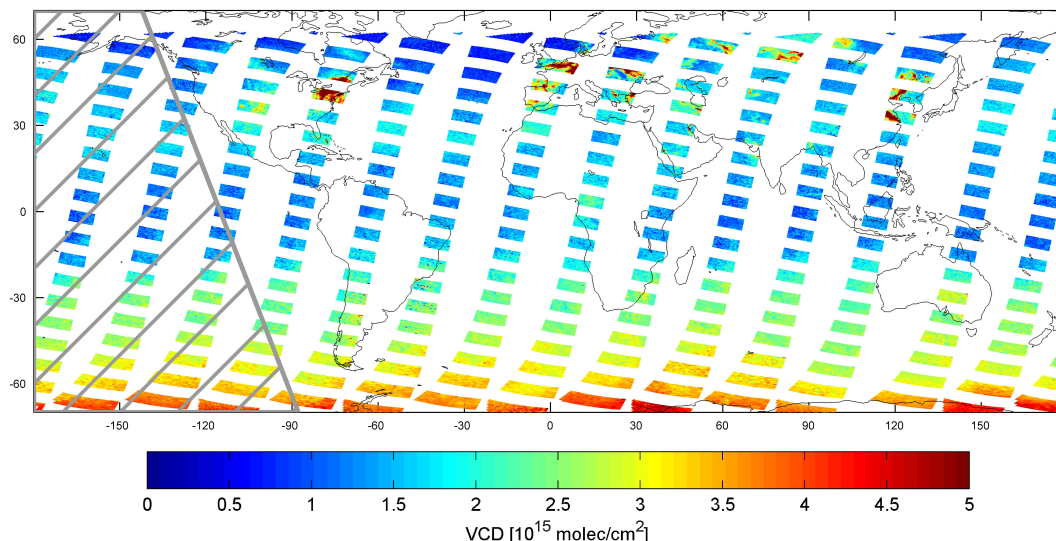


**Fig. 1.** Nadir VCD  $V^*$  for 28 January 2006. The marked area in the Pacific is the reference sector used in this study.

## 2.4 Stratospheric estimation schemes (SES)

The DOAS algorithm as described in Sect. 2.1 yields total SCDs  $S$  of NO<sub>2</sub> from the nadir measurements. The slant column density  $S$  is the concentration integrated along the effective light path. It is usually converted into a vertical column density (VCD)  $V$ , i.e. the vertically integrated concentration, via the air mass factor (AMF)  $A$ :

$$V = S/A. \quad (1)$$

The air mass factor has to be calculated by radiative transfer models and depends on observation geometry (SZA and Line-of-sight zenith angle LZA), ground albedo, aerosols, clouds, and the trace gas profile. The dominant dependencies are fundamentally different for stratospheric and tropospheric trace gases. For the considered nadir observations with SZA below 80°, stratospheric AMFs mainly depend on observation geometry and are thus well determined. Tropospheric AMFs, however, critically depend on ground albedo, clouds, aerosols, and the tropospheric trace gas profile, i.e. several parameters that have to be considered as external input.

In this study, we focus on quantifying the effect of different stratospheric estimation schemes (SES) on tropospheric column densities. For this purpose, we define  $V^*$  by applying stratospheric AMFs to the total SCDs:

$$V^* := S/A_{\text{Strat}}, \quad (2)$$

where stratospheric AMFs  $A_{\text{Strat}}$  are calculated as function of SZA and LZA using the RTM McArtim (Deutschmann, 2009) for one representative stratospheric profile of NO<sub>2</sub> with a concentration peak at 25 km. (If, instead, the actual limb profiles would be used, the resulting stratospheric

AMFs deviate less than 0.3% for SZAs up to 70°, and less than 1% for SZAs up to 80°.)

The asterisk indicates that these VCDs cannot be interpreted quantitatively as total VCDs, since the tropospheric fraction of the SCD was converted (inappropriately) with a stratospheric AMF. This has to be kept in mind for the interpretation of tropospheric residues and will be corrected below (2.5) by multiplication with  $A_{\text{Strat}}$ , yielding tropospheric SCDs.

### 2.4.1 Reference sector method (RSM)

The basic idea of the simple RSM is that the stratospheric VCD at any place can be estimated by the total VCD over a remote region (typically the Pacific) of the same latitude. I.e. the RSM assumes that (1) a sufficiently clean reference sector (RS) with negligible tropospheric pollution can be defined, and (2) the global stratospheric VCD field does only depend on latitude  $\Lambda$ , but not on longitude  $\Phi$ .

We follow this simple approach by defining a RS in the Pacific as indicated in Fig. 1, showing  $V^*$  for 28 January 2006 (additional examples for other days are shown in the Supplement). For every day  $d$ , we calculate a look-up table (LUT)  $V_{\text{RS}}^*(d, \Lambda)$  by averaging the daily measurements  $V^*$  over the RS in latitudinal bins of 1° resolution.

A smoothed LUT  $\widehat{V}_{\text{RS}}^*(d, \Lambda)$  is derived by convoluting  $V_{\text{RS}}^*(d, \Lambda)$  with Gaussian functions both in temporal ( $\sigma = 5$  days) and in latitudinal ( $\sigma = 5^\circ$ ) dimension. Both the non-smoothed ( $V_{\text{RS}}^*(d, \Lambda)$ ) and the smoothed LUT  $\widehat{V}_{\text{RS}}^*(d, \Lambda)$  are shown in Fig. S1 of the Supplement.

For the sample day 28 January 2006,  $V_{\text{RS}}^*$  and  $\widehat{V}_{\text{RS}}^*$  are also displayed as a function of latitude in Fig. 3 in direct comparison to the limb VCDs in the RS (see next section).

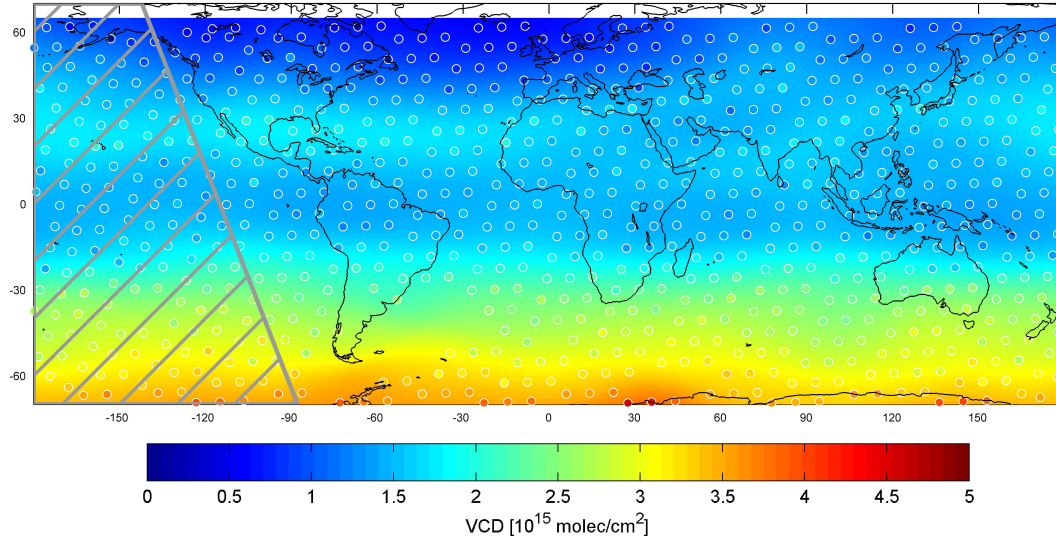


**Fig. 2.** Stratospheric VCD  $L$  derived from integrated limb profiles 27–29 January 2006. Colour-coded disks indicate the location of the tangent points for the individual limb VCDs  $L$ , the map shows the interpolated and smoothed field  $\widehat{L}(d, \Lambda, \phi)$ .

For the RSM, we define the stratospheric VCD  $W_{\text{RSM}}$  as function of day  $d$  and latitude  $\Lambda$  as:

$$W_{\text{RSM}}(d, \Lambda) := \widehat{V}_{\text{RS}}^*(d, \Lambda). \quad (3)$$

#### 2.4.2 Absolute limb correction (ALC)

Stratospheric limb VCDs (LVCDs)  $L$  are calculated from the derived limb concentration profiles (see Sect. 2.2) by simply integrating the profiles from 15 km to 42 km. Varying the lower integration limit between 12 km and 18 km affects the resulting LVCDs by less than 5%. We therefore neglect the latitudinal variation of tropopause height in this study. Errors of  $L$  are derived from integrating the uncertainties of the concentration in each layer as derived by the limb inversion. A LVCD error threshold of  $0.25 \times 10^{15} \text{ molec/cm}^2$  is defined to eliminate outliers, which mainly occur due to the South Atlantic Anomaly, a depression in the Earth's magnetic field (Van Allen belt).

Due to the co-adding of the four horizontal limb scans, one limb VCD  $L$  is available per limb state. On account of the alternating limb/nadir measurements, a single  $L$  could be used as (constant) stratospheric estimation for all measurements within the according nadir state, as in Sierk et al. (2006). However, in doing so, a single biased  $L$  would affect a complete nadir state. In addition, the assumption of a constant stratosphere within one nadir state leads to artificial step functions in the latitudinal dependency of the resulting TSCDs. Instead, we define a smoothed LUT  $\widehat{L}(d, \Lambda, \Phi)$  by folding the limb VCDs  $L$  with Gaussian functions  $G(\sigma_{\text{lon}}, \sigma_{\text{lat}})$ , where  $\sigma_{\text{lon}} = 20^\circ \times \cos(\Lambda)$  and  $\sigma_{\text{lat}} = 10^\circ \approx 1000 \text{ km}$ . These settings for  $\sigma_{\text{lon}}$  force smooth spatial patterns for low latitudes ( $\sigma_{\text{lon}} = 20^\circ \approx 2000 \text{ km}$  at the

equator), but allow for strong longitudinal gradients at higher latitudes ( $\sigma_{\text{lon}} = 10^\circ \approx 500 \text{ km}$  at  $60^\circ$  latitude), which is particularly necessary at the polar vortex.

To improve statistics and to avoid large spatial gaps, limb measurements of the previous and following day are included with half weight in the folding procedure. In addition, all limb CDs are weighted by the inverse square of their error.

Figure 2 shows a global map of limb VCDs on 28 January 2006. The location of the limb tangent points of individual LVCDs are marked by colour-coded disks, while the background map displays the smoothed LUT  $\widehat{L}(d, \Lambda, \Phi)$ . Keep in mind that for the retrieval of the profile at the tangent point, all limb scans within the limb state, covering an area of about one thousand km extent both in latitudinal as in longitudinal direction, are used for the inversion. The latitudinal dependency of  $L$  selected over the RS on 28 January 2006 is added in Fig. 3 for an absolute comparison to the RS VCDs  $V_{\text{RS}}^*$  from nadir observations.

For the absolute limb correction scheme, we define the stratospheric VCD as

$$W_{\text{ALC}}(d, \Lambda, \Phi) := \widehat{L}(d, \Lambda, \Phi). \quad (4)$$

#### 2.4.3 Relative limb correction (RLC)

The latitudinal dependencies of  $L_{\text{RS}}$  and  $V_{\text{RS}}^*$ , i.e.  $W_{\text{RSM}}$  and  $W_{\text{ALC}}$  over the reference sector, are quite similar in general, as depicted in Fig. 3, but deviate systematically in certain latitude ranges. As will be shown below, this leads to non-realistic zonal bands in the corresponding tropospheric CD product. In particular,  $L$  is often higher than  $V^*$ , leading to negative tropospheric CDs.

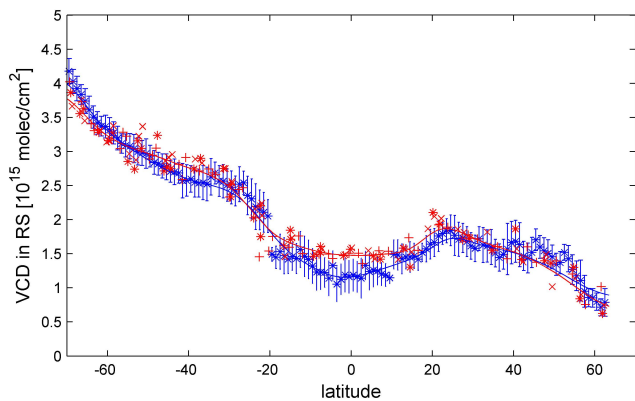


**Fig. 3.** Latitudinal dependencies of  $V_{RS}^*$  (blue) and  $L_{RS}$  (red). Nadir measurements are binned in  $1^\circ$  bins and displayed as mean (\*) and standard deviation (bar). Limb measurements are displayed for January 27 (+), 28 (\*), and 29 (x), 2006. The curves show the smoothed LUTs  $\widehat{V}_{RS}(d, \Lambda)$  (blue) and  $\widehat{L}_{RS}(d, \Lambda)$  (red).

Thus, we also perform a *relative* limb correction, which by definition eliminates the deviations of limb and nadir VCDs in the RS. The basic idea is to apply the same RS correction that was applied for the nadir VCDs also to the limb VCDs: from the limb VCDs  $L$  over the RS we derive a LUT  $\widehat{L}_{RS}(d, \Lambda)$  by smoothing over time and latitude. The difference of  $L$  and  $\widehat{L}_{RS}$  at the same day and latitude holds information on longitudinal variations for a given latitude:

$$\Delta L(d, \Lambda, \Phi) = L(d, \Lambda, \Phi) - \widehat{L}_{RS}(d, \Lambda). \quad (5)$$

We denote  $\Delta L$  as Limb Longitudinal Variation (LLV). Figure 4 displays the individual  $\Delta L$  at the limb tangent points as disks, while the background map shows  $\widehat{\Delta L}$  which is obtained by smoothing with the same settings as  $\widehat{L}$  (see Sect. 2.4.2). Again, measurements of the previous and following day are included with half weight.

Now we use the LLV  $\widehat{\Delta L}$  to refine the classical RSM and define the stratospheric VCD from relative limb correction (RLC) as

$$W_{RLC}(d, \Lambda, \Phi) := W_{RSM}(d, \Lambda) + \widehat{\Delta L}(d, \Lambda, \Phi). \quad (6)$$

Figure 5 compares global maps of stratospheric VCDs  $W$  for the three SES for 28 January 2006.

## 2.5 Tropospheric SCDs of NO<sub>2</sub>

With any of these estimates  $W$  (i.e.  $W_{RSM}$ ,  $W_{RLC}$ , or  $W_{ALC}$ ) for stratospheric VCDs of NO<sub>2</sub>, we define the tropospheric residue as

$$\Delta V^* := V^* - W. \quad (7)$$

$\Delta V^*$  represents the *tropospheric* VCD derived with a *stratospheric* AMF. Due to the strong dependency of  $A_{Strat}$  on observation geometry,  $\Delta V^*$  strongly depends on

SZA and LZA, which is not realistic for tropospheric VCDs. To correct this inconsistency, we transfer  $\Delta V^*$  back to a tropospheric *slant* column density (TSCD)  $T$ :

$$T := \Delta V^* \times A_{Strat}. \quad (8)$$

From  $T$ , a tropospheric VCD can be derived directly by applying the appropriate tropospheric AMF (and a temperature correction to account for the “cold” NO<sub>2</sub> cross-section at 220 K used in the DOAS-fit, see Sect. 2.2). Within this study, however, we do not apply tropospheric AMFs, since we want to focus solely on the effect of different SES, without involving (and discussing the impact of) external datasets (for ground albedo, clouds/aerosols and profiles). For orientation, however, note that tropospheric AMFs for cloud free scenes are of the order of 1 (Richter and Burrows, 2002), and generally  $<1$  for clouded scenes, except for cases with substantial NO<sub>2</sub> within/above the cloud.

All total CDs ( $V^*$ ) and all stratospheric CDs ( $W$ ) presented in this study are vertical column densities, whereas the tropospheric CDs  $T$  discussed below are slant column densities. This differentiation is potentially confusing, but necessary, since stratospheric CDs need to be processed in terms of VCDs (e.g. for the averaging of RS column densities of the same latitude for different SZA/LZA), but the relevant tropospheric CDs, prior to the application of tropospheric AMFs, are slant column densities. Thus, we discuss the effect of the different SES on tropospheric CDs in terms of SCDs in Sects. 3 and 4. The stratospheric AMF, i.e. the ratio of  $T$  and  $\Delta V^*$ , is slightly above 2 for low SZA (tropics) up to 7 for high SZA ( $80^\circ$ ).

The resulting TSCDs for the three different SES are displayed in Fig. 6.

## 2.6 Intrinsic error information

In this section we briefly discuss the potential of detecting and estimating systematic as well as statistical errors from the measurements themselves. A more detailed discussion of this issue and the actual definition of the terms we use for quantitative error information are given in Sect. S3 of the Supplement.

Estimates of the accuracy of TSCDs can be derived from the TSCDs themselves in so far that systematic negative TSCDs (on a level beyond possible statistical fluctuations around zero) are definitively unphysical. Also, strange spatial patterns of TSCDs far from known NO<sub>x</sub> sources may indicate shortcomings of the SES. Finally, if a SES is insufficient, fluctuations of the remaining stratospheric features lead to enhanced standard deviations (over time) of the resulting TSCDs. Thus, the success of an advanced SES has to be demonstrated by an improvement of accuracies, i.e. the removal/reduction of a) systematic negative TSCDs, b) strange spatial features which are obviously not of tropospheric origin, and c) TSCD standard deviations (over time).

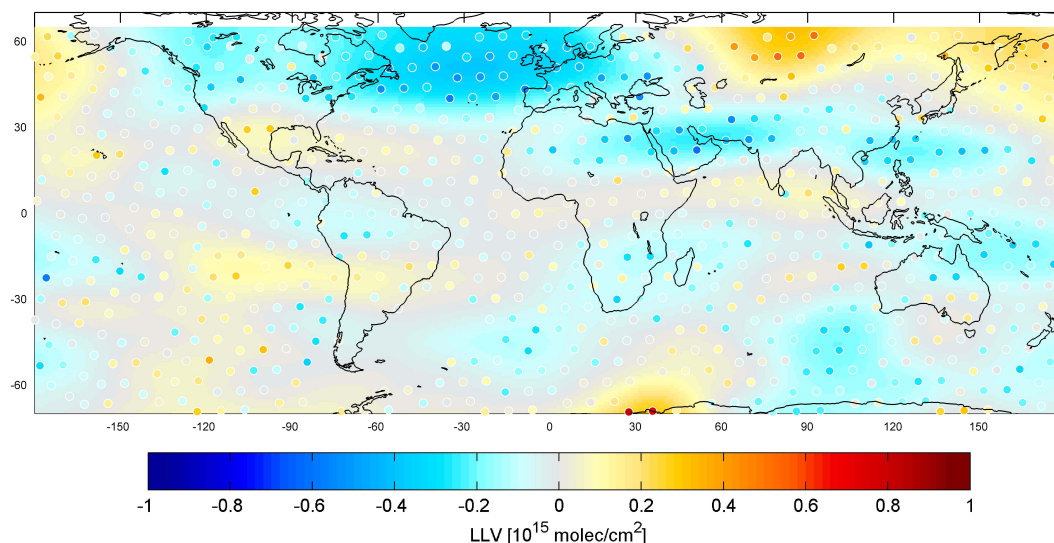


**Fig. 4.** Longitudinal Limb Variation (LLV)  $\Delta L$  for 28 January 2006. Disks show the LLV for the individual limb states ( $\Delta L$ ), the map shows the interpolated and smoothed field  $\widehat{\Delta L}(d, \Lambda, \Phi)$ .

Additional information on both statistical and systematic errors can be derived from the standard deviation (over longitude) of  $W$  in the reference sector. This quantity comprises statistical errors (e.g. from the DOAS fit error and natural fluctuations of stratospheric VCDs), but enhanced values clearly indicate additional systematic errors, e.g. due to fit artefacts over oligotrophic oceanic regions.

From the comparison of individual LLV  $\Delta L$  to the smoothed LUT  $\widehat{\Delta L}$ , information on the performance of the smoothing/interpolation procedure can be derived, mainly in cases of strong temporal and spatial gradients.

In Sect. S3 of the Supplement, we define and display the error quantities  $\delta W_{\text{RSM}}$  and  $\delta W_{\text{RLC}}$ , which are automatically calculated during the TSCD retrieval, and are provided as function of day and latitude. Thus, although shortcomings of the RLC remain for some regions and times, these can be recognized by enhanced values of  $\delta W_{\text{RSM}}$  or  $\delta W_{\text{RLC}}$ .

### 3 Results

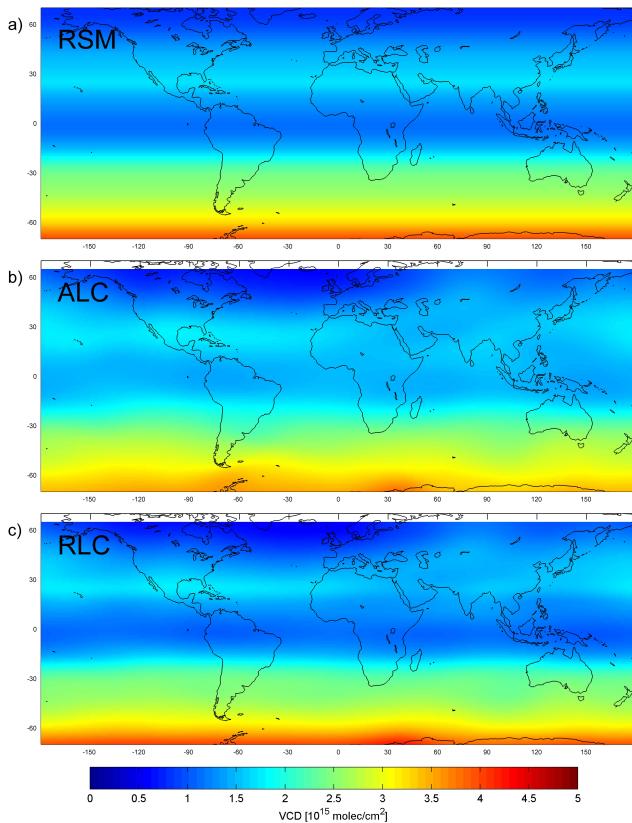
In this section, we present TSCDs for the different SES, and analyze their specific characteristics and differences. Again, we focus on wintertime, where the shortcomings of the RSM become particularly evident. Results for other times of the year are presented in the Supplement and also shortly discussed below.

Figure 6 exemplarily shows the resulting TSCDs  $T_{\text{RSM}}$ ,  $T_{\text{ALC}}$ , and  $T_{\text{RLC}}$  for 28 January 2006. Note that the colorscale has been chosen to accentuate small systematic deviations from 0 – in particular negative ones – over “clean” regions. Polluted regions like Europe, the east coast of the United States, or China, are by far in saturation.

As can be seen in Fig. 4, the simple assumption of a zonally constant stratospheric CD is not valid. As a consequence, the RSM leads to – unphysical – negative TSCDs  $T_{\text{RSM}}$  (Fig. 6a) over the Northern Atlantic down to  $-2 \times 10^{15}$  molec/cm<sup>2</sup>, which is far below the statistical uncertainty. In contrast,  $T_{\text{RSM}}$  over wide areas in remote Northern Asia is quite high. Similar shortcomings of the RSM in wintertime have been discussed in, e.g. Richter and Burrows (2002) or Sierk et al. (2006).

The ALC (Fig. 6b) significantly improves the patterns over the Northern Atlantic, and the strong negative bias is successfully corrected. However,  $T_{\text{ALC}}$  shows strong latitudinal features, both positive and negative: oceanic CDs around the equator are negative now (in contrast to  $T_{\text{RSM}}$ ) about  $-1 \times 10^{15}$  molec/cm<sup>2</sup>, and  $T_{\text{ALC}}$  is unrealistically high ( $2 \times 10^{15}$  molec/cm<sup>2</sup>) south of 60° S, i.e. far from any known source of NO<sub>x</sub>. This is a direct consequence of the different latitudinal dependencies of  $V_{\text{RS}}^*$  and  $L_{\text{RS}}$  (Fig. 3), which reveals systematic deviations that lead to negative (20° S to 20° N) as well as positive (south of 60° S) background TSCDs  $T_{\text{ALC}}$ . Keep in mind that Fig. 3 displays VCDs; the differences in TSCD (Fig. 6b) are higher by the stratospheric AMF  $A_{\text{Strat}}$ , which varies from about 2 in the tropics up to 7 at high latitudes.

The RLC results in the most plausible NO<sub>2</sub> TSCDs (Fig. 6c).  $T_{\text{RLC}}$  shows a clear improvement of spatial patterns compared to  $T_{\text{RSM}}$ : the negative  $T_{\text{RSM}}$  over the Northern Atlantic are corrected in  $T_{\text{RLC}}$ , and also other regions with negative  $T_{\text{RSM}}$  (e.g. southeast of Japan) are more plausible in  $T_{\text{RLC}}$ . At the same time, the artificial zonal features introduced by the ALC are eliminated by the RLC: in contrast to  $T_{\text{ALC}}$ ,  $T_{\text{RLC}}$  is – per definition – still 0 on average over the RS.



**Fig. 5.** Stratospheric VCDs  $W$  on 28 January 2006 for the different stratospheric estimation schemes: (a) reference sector method, (b) absolute limb correction, and (c) relative limb correction.

The longitudinal variations in  $T_{RSM}$  at about  $60^\circ$  S are reduced in  $T_{RLC}$ , but could not be removed completely by the RLC. Generally, patterns at Northern hemispheric (NH) mid- and high latitudes are corrected successfully by the RLC, but are only lessened in the Southern Hemisphere (SH), as illustrated by the additional examples given in the Supplement, and discussed in Sect. 4.

After illustrating the different TSCDs for a specific day, we compare monthly climatologies (mean 2003–2008) of TSCDs for January (Fig. 7) and additional months in the Supplement (Figs. S11–S16). Obviously, the longitudinal variations of stratospheric NO<sub>2</sub>, as observed for 28 January 2006, do not cancel out by temporal averaging, but instead systematic spatial patterns stand out.

Mean January  $T_{RSM}$  (Fig. 7) is negative down to  $-2 \times 10^{15}$  molec/cm<sup>2</sup> over large parts of Canada and the Northern Atlantic, and quite high ( $> 1 \times 10^{15}$  molec/cm<sup>2</sup>) throughout northeastern Russia. Like for the single day sample (Fig. 6), the ALC reduces/removes these longitudinal variations, but introduces zonal stripes of negative TSCDs around the equator, and high positive TSCDs south of  $60^\circ$  S (Fig. 7b). Again,  $T_{RLC}$  improves the longitudinal variations while retaining the RS levels to 0 on average (Fig. 7c).

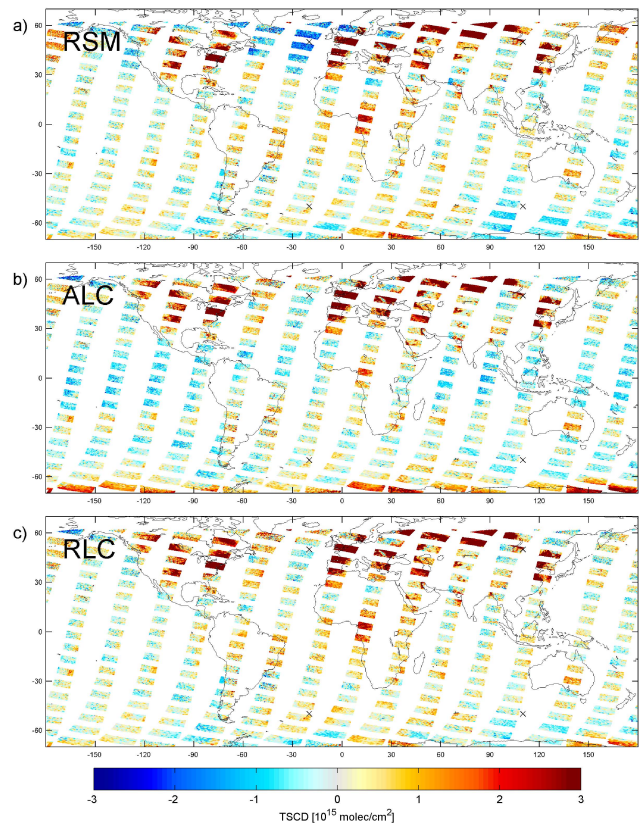


**Fig. 6.** Tropospheric SCDs for 28 January 2006. (a)  $T_{RSM}$ : reference sector method. (b)  $T_{ALC}$ : absolute limb correction. (c)  $T_{RLC}$ : relative limb correction. Crosses mark the locations considered in the time-series analysis (see Figs. 11–12).

The differences of the mean TSCDs are shown in Fig. 8, directly illustrating the effects of the different stratospheric estimation schemes. Compared to RSM, both ALC (Fig. 8a) and RLC (Fig. 8b) remove a dipolar pattern with a maximum amplitude of  $2.5 \times 10^{15}$  molec/cm<sup>2</sup> at northern latitudes. However, the ALC introduces zonal stripes in the climatology up to  $1.2 \times 10^{15}$  molec/cm<sup>2</sup> over the RS at the equator (Fig. 8a and c). In contrast, the difference  $T_{RSM} - T_{RLC}$  is negligible for latitudes between  $30^\circ$  N and  $60^\circ$  S.

Note that  $T_{ALC}$  and  $T_{RLC}$  show different longitudinal dependencies (see the local pattern over South America in Fig. 8c), which would on first view not be expected, since the longitudinal dependencies of both,  $W_{ALC}$  and  $W_{RLC}$ , are derived from the limb measurements only. The reason for the observed differences in longitudinal behaviour is the calculation of  $\widehat{\Delta V}$ , which is derived from smoothing the individual  $\Delta V$ , instead of performing the RS correction to  $\widehat{V}$ ; this is a non-commutative procedure. The difference over South America stands out, because most limb observations are skipped there as a consequence of high errors of  $L$  due to the South Atlantic Anomaly.

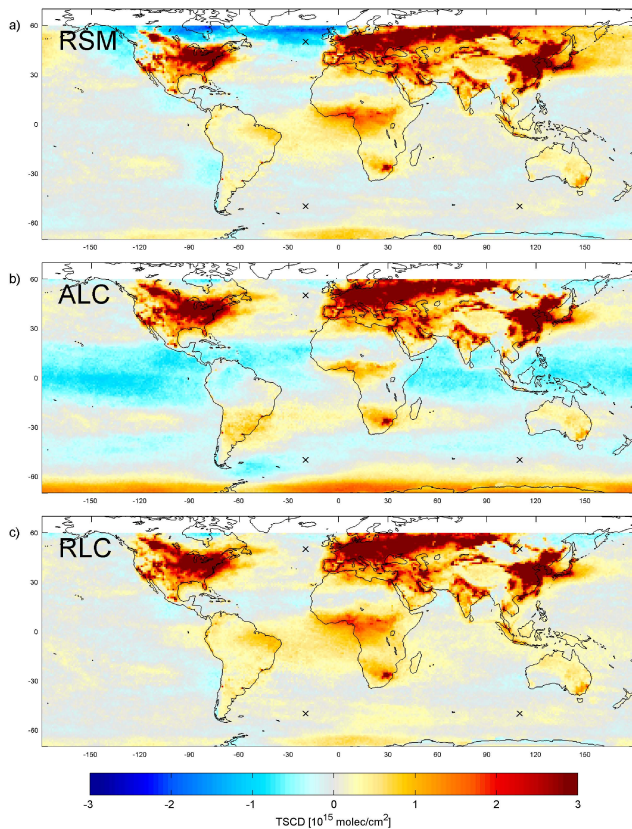


**Fig. 7.** Mean tropospheric SCDs for January 2003–2008. (a)  $T_{\text{RSM}}$ : reference sector method. (b)  $T_{\text{ALC}}$ : absolute limb correction. (c)  $T_{\text{RLC}}$ : relative limb correction.

Aside from the effect of the different SES on mean values, we also analyzed the standard deviations  $s$  of TSCDs over time for January 2003–2008 (Fig. 9). As expected, standard deviations are generally high over polluted regions, where mean TSCDs are enhanced, due to variability of tropospheric CDs. Beyond that,  $s(T_{\text{RSM}})$  is high ( $> 3 \times 10^{15}$  molec/cm<sup>2</sup>) over the Northern Atlantic, in contrast to  $s(T_{\text{ALC}})$  and  $s(T_{\text{RLC}})$ . Figure 10, which shows the differences of standard deviations, reveals that both  $T_{\text{ALC}}$  and  $T_{\text{RLC}}$  lead to lower standard deviations over large areas at high latitudes. The consideration of longitudinal variations from limb measurements thus clearly reduces the standard deviations by about 1 up to  $3 \times 10^{15}$  molec/cm<sup>2</sup> compared to the simple RSM. Note that standard deviations of  $T_{\text{ALC}}$  and  $T_{\text{RLC}}$  are almost identical (Fig. 10c), despite their differences in mean values. This indicates that  $s(T_{\text{ALC}})$  is driven by tropospheric variability and stratospheric dynamics, but *not* by the zonal stripes introduced by the ALC, which are thus rather constant in magnitude and location for a fixed month.

Figures S4–S16 of the Supplement illustrate that the RLC also improves the spatial patterns, both on individual days as well as in monthly climatologies, for other times of the year. Typical values for daily LLVs (in terms of VCD) are below

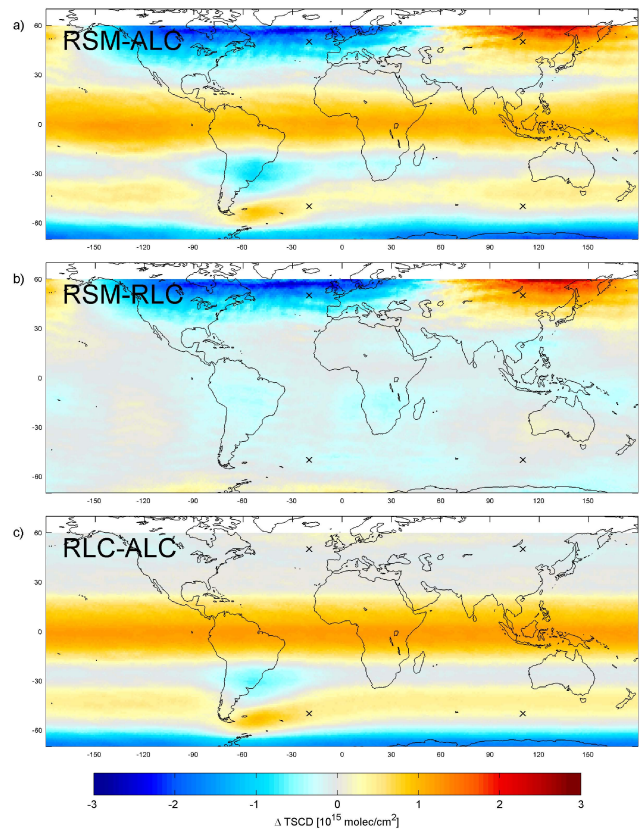
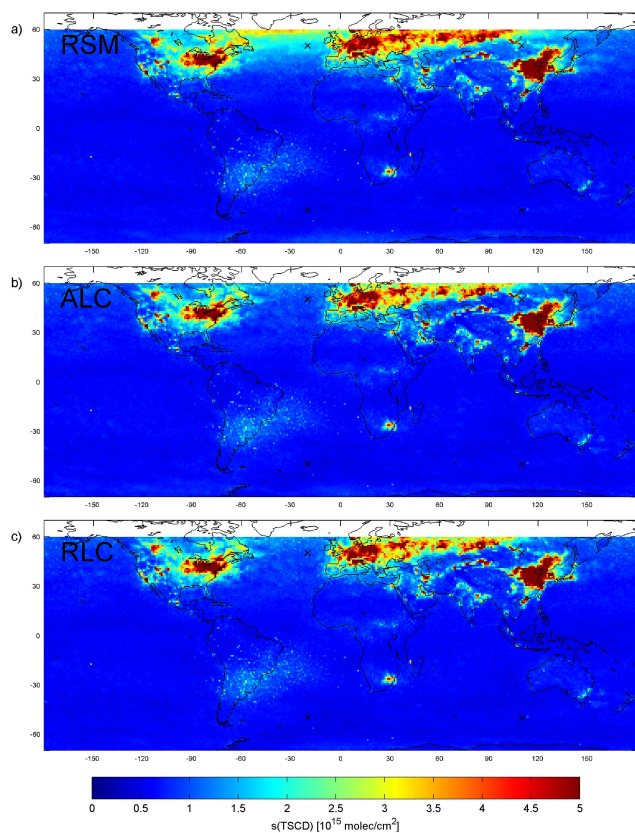


**Fig. 8.** Difference of mean tropospheric SCDs  $T_{\text{RSM}} - T_{\text{ALC}}$  (a),  $T_{\text{RSM}} - T_{\text{RLC}}$  (b), and  $T_{\text{RLC}} - T_{\text{ALC}}$  (c) for January 2003–2008.

$\pm 0.3 \times 10^{15}$  molec/cm<sup>2</sup> for low latitudes, but can reach  $\pm 0.6$  up to  $1 \times 10^{15}$  molec/cm<sup>2</sup> for higher latitudes in some months (Figs. S4, S6, S8). Figure S10 illustrates that the principal shortcoming of the ALC, caused by different latitudinal dependencies of  $V^*$  and  $L$ , with  $L$  being generally higher than  $V^*$ , is present throughout the year.

For the monthly climatologies, the RLC modifies the resulting TSCDs by less than  $0.5 \times 10^{15}$  molec/cm<sup>2</sup> for low and midlatitudes, and up to  $1 \times 10^{15}$  molec/cm<sup>2</sup> at high northern latitudes (about 60°) in April and October. In October, the difference  $T_{\text{RSM}} - T_{\text{RLC}}$  is up to  $3 \times 10^{15}$  molec/cm<sup>2</sup> at 60° S, and still unrealistic spatial patterns (negative  $T_{\text{RLC}}$ ) are present (Figs. S15–S16). Thus, especially for the SH, the RLC sometimes reduces, rather than completely eliminates the artefacts of the RSM. Nevertheless, standard deviations of  $T_{\text{RSM}}$  are always significantly reduced by the RLC (Figs. S12, S14, S16).

After discussing global maps of TSCDs for the different SES for different days and months, we also investigate the temporal pattern and frequency distributions of TSCDs for four selected locations: two in the NH (50° N) and two in the SH (50° S) at 20° W and 110° E, respectively. All locations are remote, far from known sources of NO<sub>x</sub>, and are considered to be “clean”. They are marked by crosses in Figs. 6–10.



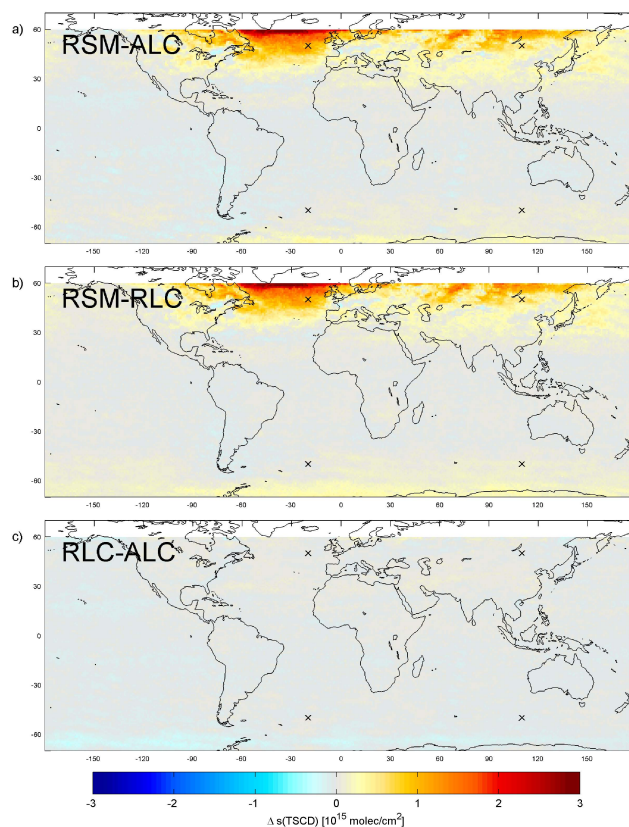
**Fig. 9.** Standard deviations of tropospheric SCDs for January 2003–2008. (a)  $s(T_{\text{RSM}})$ , (b)  $s(T_{\text{ALC}})$ , (c)  $s(T_{\text{RLC}})$ .

Figure 11 shows the annual cycles of the different TSCDs. Figure 12 displays the respective frequency distributions and lists means and standard deviations for these four locations.

The first location (20° W, 50° N) is located in the Northern Atlantic.  $T_{\text{RSM}}$  (blue) is often negative and generally show a high variability in winter. This variability is reduced both in  $T_{\text{ALC}}$  (green) and  $T_{\text{RLC}}$  (orange). However,  $T_{\text{ALC}}$  shows systematically higher CDs in summer. While the mean of  $T_{\text{RSM}}$  is negative,  $T_{\text{RLC}}$  is almost zero on average. The standard deviations both of  $T_{\text{ALC}}$  and  $T_{\text{RLC}}$  are reduced compared to  $T_{\text{RSM}}$ .

At the second location, placed in Russia (110° E, 50° N) far from large cities, wintertime  $T_{\text{RSM}}$  is quite high (up to  $5 \times 10^{15}$ ). On average,  $T_{\text{RSM}}$  is  $0.67 \times 10^{15} \text{ molec/cm}^2$ . ALC reduces these high wintertime TSCDs, but introduces too high TSCDs in summertime.  $T_{\text{RLC}}$  is close to zero on average and has a reduced standard deviation.

The SH locations, (20° W and 110° E, 50° S) are over Ocean, far from known NO<sub>x</sub> sources. The annual cycle and frequency distributions of both southern locations are similar:  $T_{\text{RSM}}$  shows high variability and high CDs in SH winter (NH summer). ALC overcorrects the SH wintertime TSCDs, resulting in negative  $T_{\text{ALC}}$  down to  $-5 \times 10^{15} \text{ molec/cm}^2$ . Again,  $T_{\text{RLC}}$  is close to zero on average and has a reduced standard deviation.



**Fig. 10.** Difference of the standard deviations of tropospheric SCDs  $s(T_{\text{RSM}}) - s(T_{\text{ALC}})$  (a),  $s(T_{\text{RSM}}) - s(T_{\text{RLC}})$  (b), and  $s(T_{\text{RLC}}) - s(T_{\text{ALC}})$  (c) for January 2003–2008.

For all considered clean locations, the mean of  $T_{\text{RLC}}$  is non-negative, close to zero, and its standard deviation is lowest, indicating that RLC is the most realistic SES.

#### 4 Discussion

Estimating the stratospheric column density over a remote reference sector is an easy, robust method for the retrieval of tropospheric CDs, and has been used successfully in several studies on tropospheric NO<sub>2</sub>. In particular, it implies a first-order correction of any systematic offset in total CDs. The simple assumption of zonal constancy, however, clearly fails at higher latitudes, in particular close to the polar vortex. We present two advanced stratospheric estimation schemes (ALC and RLC) involving additional limb measurements and apply them to 6 years of SCIAMACHY measurements.

From the individual limb profiles (one per SCIAMACHY state), daily global maps of  $\hat{L}$  and  $\hat{\Delta L}$  are compiled by spatial and temporal interpolation and smoothing. For strong spatial gradients, as well as for strong day-to-day changes of spatial patterns, the estimated LUTs  $\hat{L}$  and  $\hat{\Delta L}$  are thus not appropriate. However, on average, over- and underestimations are expected to cancel each other out.

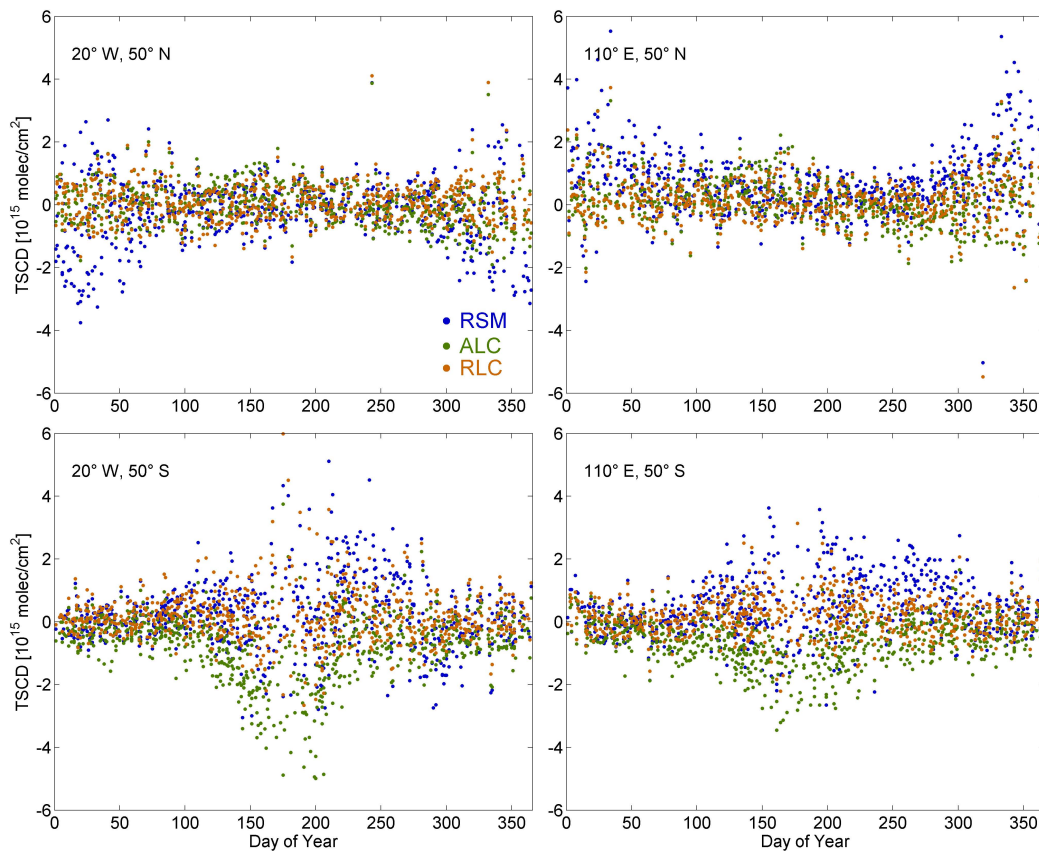


**Fig. 11.** Annual cycle of TSCDs for four selected locations (as marked in Figs. 6–10). Upper row: 50° N. Lower row: 50° S. Left column: 20° W. Right column: 110° E. The different schemes are marked by colors: blue ( $T_{\text{RSM}}$ ), green ( $T_{\text{ALC}}$ ), and orange ( $T_{\text{RLC}}$ ).

Stratospheric correction by ALC generally improves spatial patterns of TSCDs compared to the RSM with respect to longitudinal variations. However, in the resulting TSCDs  $T_{\text{ALC}}$ , systematic zonal stripes (about  $\pm 1 \times 10^{15}$  molec/cm<sup>2</sup> in monthly climatologies) show up as a consequence of different latitudinal dependencies of  $V_{\text{RS}}^*$  and  $L_{\text{RS}}$ . Generally,  $L$  is *higher* than  $V^*$  for low/mid latitudes most time of the year, resulting in negative  $T_{\text{ALC}}$ . Low or even negative tropospheric CDs, resulting from subtraction of stratospheric limb VCDs, can also be seen in Sioris et al. (2004) (Fig. 6 therein) and in PROMOTE (2004).

The following aspects might lead to systematic biases in nadir and/or limb data, thus potentially causing different latitudinal dependencies:

- The DOAS retrievals for nadir and limb use different cross-sections for NO<sub>2</sub> (see Sects. 2.2 and 2.3). As a consequence, limb CDs are systematically higher (compared to a fit using the NO<sub>2</sub> cross-section from Vandaele et al., 1998) by about 4%. In addition, total nadir SCDs might be biased due to artificial spectral structures in the direct solar reference measurement, caused by the optical system (diffusor plate). However, the observed zonal stripes can not be eliminated, neither by re-scaling nor by simply adding a constant offset to total SCDs.
- In our analysis, we define the limb VCD  $L$  as the integrated limb concentration from 15 km to 42 km. We thereby neglect latitudinal variations of the tropopause height (TH), and thus generally tend to overestimate  $L$  over the tropics, and underestimate it at high latitude. We investigated the impact of the TH on  $L$  by varying it between 12 and 18 km. The resulting modifications of  $L$  are below 5%, corresponding to absolute values of 0.05 to  $0.25 \times 10^{15}$  molec/cm<sup>2</sup>. For an absolute limb correction scheme, the fixed TH can thus lead to significant errors in the limb estimation, in particular for high latitudes. However, our choice of a fixed TH can not explain the different latitudinal dependencies of  $V^*$  and  $L$  seen in Fig. 2 and Fig. S10 of the Supplement, and the resulting zonal bands in  $T_{\text{ALC}}$ .
- Although limb and nadir measurements are performed from the same platform, there is a time shift of about 7 minutes between the limb- and the nadir sounding of the stratosphere. For high SZA (sunrise and sunset), this may be long enough for significant differences of NO<sub>2</sub> due to changes in photochemistry.
- The effects of clouds and aerosols are ignored in the retrieval of limb profiles. The neglect of high clouds

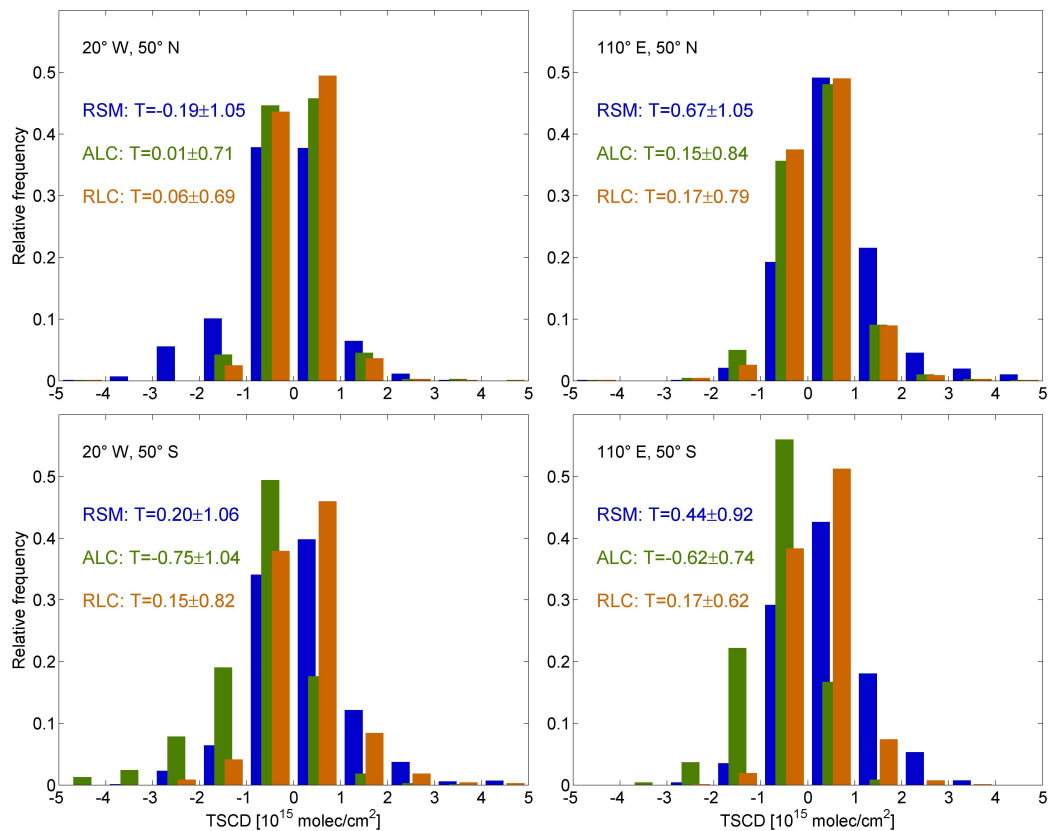


**Fig. 12.** Frequency distribution of TSCDs for four selected locations (as marked in Figs. 6–10). Upper row: 50° N. Lower row: 50° S. Left column: 20° W. Right column: 110° E. The different schemes are marked by colors: blue ( $T_{\text{RSM}}$ ), green ( $T_{\text{ALC}}$ ), and orange ( $T_{\text{RLC}}$ ). The numbers give the respective means and standard deviations (in  $10^{15}$  molec/cm<sup>2</sup>).

(e.g. over the ITCZ) results in an underestimation of box AMFs in and above the clouds. However, the total limb column would only be affected significantly, if there would be high NO<sub>2</sub> concentrations in/directly above the cloud.

- Clouds potentially affect the nadir total SCDs by their impact on the Earth shine spectra, e.g. via their impact on polarization, the probability of inelastic scattering (Ring effect), or the shielding of light reflected at the ground, carrying spectral albedo information. The latter could be important especially over the problematic oligotrophic oceanic regions. Yet, we find no correlation of TSCDs and cloud fraction ( $R = -0.01$  for 28 January 2006, over the RS).
- In addition, clouds lead to increased stratospheric AMFs, which is only a small effect ( $< 2\%$  difference between  $A_{\text{Strat}}$  for cloud-free versus clouded conditions, as calculated with McArtim), and thus not considered in this study.
- The limb inversion scheme is based on one dimensional RTM, assuming horizontal homogeneity. In cases of horizontal gradients, this simplification leads to errors in the resulting profiles, since the effective light paths

for low tangent heights do not reach as close to the tangent point as for high tangent heights. At the Arctic polar vortex, the corresponding errors for NO<sub>2</sub> concentrations were found to be 20% on average (Puķīte et al., 2008). Currently, 3-D effects are investigated and quantified for the SH polar vortex, as well as for midlatitudes and tropics, where substantial latitudinal gradients can also occur (Puķīte et al., 2010). This study uses measurements of successive orbits in exclusive limb geometry in December 2008, following the SCIAMACHY operation change request OCR #38). Total errors of integrated VCDs are of the order of  $0.1 \times 10^{15}$  molec/cm<sup>2</sup> for strong horizontal gradients. But though the simplification of a 1-D retrieval results in systematic errors, those can not explain the particular differences in the latitudinal dependencies of  $V^*$  and  $L$ .

These and possibly other factors with latitudinal dependency (which may also be the consequence of a SZA dependency) have potentially systematic impact on  $V^*$  and/or  $L$ . However, none of the reasons discussed above could conclusively explain the observed deviations of  $V^*$  and  $L$  over the RS. The in-detail comparison of the latitudinal dependencies of  $V^*$  and  $L$  thus can help to indicate and quantify

shortcomings of the nadir and/or limb retrievals in future studies. But at present, as shown in this study, the direct ALC is not appropriate for an automatized retrieval of NO<sub>2</sub> TSCDs.

A third method, the RLC, was quite successful in removing longitudinal variations without the drawbacks of the ALC. By applying the RSM to nadir and limb data alike, an absolute calibration of vertical column densities (limb and nadir) is not required, and systematic biases are first-order corrected. Also possible jumps in the time series (due to, e.g. calibration setting changes) and degradation effects are automatically corrected for. The RLC thus keeps the heritage of the RSM, i.e. being a simple, robust, and model-independent correction scheme, but clearly improves spatial patterns of the resulting TSCDs, where longitudinal variation causes the RSM to fail. Over clean regions, mean  $T_{RLC}$  is generally close to 0, and its standard deviation is the lowest of all SES. The RLC introduces changes in TSCD (compared to RSM) up to  $3 \times 10^{15}$  molec/cm<sup>2</sup> for some months (January, Fig. 8b; October, Fig. S16a in the Supplement), while in NH summer, changes are generally low ( $< 0.5 \times 10^{15}$  molec/cm<sup>2</sup> for July, Fig. S14a in the Supplement).

Although the RLC is a significant improvement over the simple RSM, it is not capable of eliminating stratospheric features completely. In particular for the SH, spatial patterns that are obviously not of tropospheric origin remain in maps of  $T_{RLC}$ . Possible reasons for these pronounced SH shortcomings are:

- Especially in the SH, very localized stratospheric features occur. For instance, on 24 October 2005, a small filament of enhanced NO<sub>2</sub> CDs is visible in the map of  $V^*$  south of Africa (see Figs. S8 and S9 of the Supplement). Limb VCDs  $L$  for this region are also enhanced, i.e. the observed NO<sub>2</sub> is located in the stratosphere. Although the limb measurements are capable of detecting this feature, they can not fully resolve the spatial structure of this filament due to their coarse spatial resolution (one profile per state). This inevitably leads to an incomplete correction of this structure by the RLC (see Fig. S9c). This shortcoming is reflected by a high value for  $\delta W_{RLC}$  (and thus  $\delta T_{RLC}$ ), which regularly occurs in autumn at 60°S (Fig. S3).
- As discussed above, the neglect of 3-D effects results in systematic errors: at the Arctic polar vortex (where the concentration gradient is positive in viewing direction), concentrations (and thus integrated VCDs) are underestimated, and, vice versa, at the Antarctic polar vortex, VCDs are overestimated. Thus, in particular for the SH, longitudinal variations should rather be overcompensated by applying the LLV. Hence, 3-D effects can not explain the insufficient correction for the SH.

- Limb measurements are performed in forward direction, i.e. southwards for the descending orbits. I.e. at high northern latitudes, limb measurements “look” from high to low SZA, with the sun ahead, and vice versa at high southern latitudes. This is a systematic difference of the observation geometries of both hemispheres which may at least partly explain why the RLC is less successful in the SH.

One remaining possible shortcoming of both RSM and RLC are systematic biases of total nadir SCDs due to spectral interference of water absorption and vibrational Raman scattering. This potentially affects the stratospheric estimation around 30° S, with impact on tropospheric CDs over southern South America, South Africa, and Australia. From the spatial variations of NO<sub>2</sub> in and outside oligotrophic oceanic regions, we estimate this bias to be below  $0.5 \times 10^{15}$  molec/cm<sup>2</sup> (in terms of TSCDs). Further improvements of the spectral fit are the purpose of ongoing studies.

While the ALC should, principally, yield “total” tropospheric CDs, the TSCDs from RSM and RLC are, by definition, tropospheric *excess* CDs w.r.t. the reference sector: the small, but existent tropospheric NO<sub>2</sub> SCDs are interpreted as stratospheric SCD. For quantitative interpretation of  $T_{RSM}$  and  $T_{RLC}$ , modelled TSCDs in the RS have to be added, which are of the order of  $0.3\text{--}0.6 \times 10^{15}$  molec/cm<sup>2</sup>, depending on latitude (Martin et al., 2002). Alternatively, for comparisons of  $T_{RLC}$  (“pure” measurement) to modelled TSCDs, the same RS correction could be applied to the latter (Franke et al., 2009).

The RSM is per definition an additive correction (Eqs. 3 and 7): The RS VCDs  $V_{RS}^*$  are subtracted from the VCDs  $V^*$ , thereby removing the stratosphere and possible additive biases. In analogy, we applied an additive RSM also to the limb data to define the LLV (see Eq. 5), and use this LLV to define the RLC (Eq. 6). In our point of view, this is the most simple and straightforward approach. A possible systematic multiplicative bias of limb or nadir measurements, however, would have to be corrected with a kind of multiplicative RLC. But at the moment, we can only speculate about reasons for the deviations of nadir and limb VCDs over the RS, making the ALC inappropriate. We thus cannot decide, from a theoretical point of view, whether an additive or a multiplicative approach is advisable (probably a combination of both). However, as long as the absolute values of nadir- and limb VCDs are of the same order of magnitude, both approaches give similar results. Since the deviations of  $V_{RS}^*$  and  $L_{RS}$  are less than 10% for high latitudes (see Fig. 3 and Fig. S10 in the Supplement), the effect of a multiplicative (instead of additive) bias approach on LLV is small. On the other hand, for low latitudes, where deviations  $V_{RS}^*$  and  $L_{RS}$  can reach up to 50% (Fig. S10 in the Supplement, July), the LLV itself is small ( $\Delta L < 0.2 \times 10^{15}$  molec/cm<sup>2</sup> for  $V$ ).

The changes in TSCDs between the different SES are significant, and have a strong impact on quantitative studies of tropospheric NO<sub>2</sub>, like emission estimates. In particular over Siberia, RLC leads to TSCDs that are lower compared to  $T_{\text{RSM}}$  by about  $1$  to  $2 \times 10^{15}$  molec/cm<sup>2</sup> in a climatology for January 2003–2008. Over Europe, on the other hand,  $T_{\text{RLC}}$  is higher than  $T_{\text{RSM}}$  by about  $1 \times 10^{15}$  molec/cm<sup>2</sup>. Over polluted European sites, mean wintertime TSCDs reach values of about  $4 \times 10^{15}$  molec/cm<sup>2</sup> (Paris) up to  $> 10 \times 10^{15}$  molec/cm<sup>2</sup> (Milan) (on a  $0.5^\circ \times 0.5^\circ$  grid), i.e. the RLC SES has significant impact on TSCDs even at polluted sites. For hemispheric spring and summer, effects are generally smaller, but still systematic differences of RSM and RLC of the order of  $0.2$ – $0.4 \times 10^{15}$  molec/cm<sup>2</sup> occur over large areas.

Though the RSM is an established SES, our study emphasizes the need to account for longitudinal variations of stratospheric NO<sub>2</sub>. This also affects studies on relative signals (e.g. the Sunday reduction of the weekly cycle), as the RSM bias is additive, not multiplicative (see Eq. 7). In studies on NO<sub>2</sub> in remote regions at high latitudes with relatively low TSCD levels, e.g. soil emission estimates over deserted regions like Siberia, the impact of the stratospheric estimation and the related uncertainties have to be kept in mind.

## 5 Conclusions

In this study, we analyzed different schemes for the estimation of stratospheric column densities (CDs) of NO<sub>2</sub>, involving limb measurements from the SCIAMACHY instrument, and the consequences for the resulting tropospheric CDs.

Estimating the stratospheric CDs by a simple reference sector method (RSM), which is generally a robust and successful method, leads to systematic errors in stratospheric CDs. Consequently, tropospheric CDs are negative over the Atlantic ( $50^\circ$  N) down to  $-4 \times 10^{15}$  (daily extreme)/ $-1 \times 10^{15}$  molec/cm<sup>2</sup> (monthly climatology) in autumn/winter months.

A direct, absolute limb correction (ALC) is capable of correcting longitudinal variations of stratospheric CDs, thus being an improvement compared to the simple reference sector method at high latitudes. However, the latitudinal dependencies of limb and nadir CDs turned out to be systematically different. Further validation of nadir CDs and limb profiles, especially at low latitudes, is needed, to investigate and eventually understand these different latitudinal dependencies, which let an automatized retrieval of tropospheric CDs by the ALC fail.

Instead, we developed a relative limb correction (RLC) scheme which successfully improves the RSM w.r.t. longitudinal features, without introducing artefacts elsewhere, and suggest using this scheme for the retrieval of tropospheric NO<sub>2</sub> CDs. The RLC keeps the heritage of the simple RSM, i.e. it is based on measurements and free of a-priori assumptions (like NO<sub>x</sub> emissions or modelled stratospheric CDs),

but significantly improves the shortcomings of the RSM. Compared to both RSM and ALS, the spatial patterns of the CDs derived by RLC are the most plausible, i.e. means are closest to zero for clean regions and standard deviations over time are the lowest.

Although the RLC generally works successfully, spatial features of stratospheric origin partly remain in tropospheric CDs, especially for high southern latitudes. Fortunately, regions south of  $50^\circ$  S are not in the focus of studies on tropospheric NO<sub>2</sub>. Nevertheless, it is of course desirable to overcome the remaining shortcomings by future improvements.

Error quantities are defined as a function of day and latitude, considering (a) the standard deviation of CDs in the RS and (b) deviations of smoothed and non-smoothed stratospheric maps. These quantities provide information on both statistical and especially systematic errors, like shortcomings of the DOAS fit over oligotrophic oceans, or scenarios with high spatial gradients of stratospheric NO<sub>2</sub> which are not resolved by the limb measurements.

The RLC was discussed for NO<sub>2</sub> in this study. In principle, it could also be applied to other trace gases like O<sub>3</sub>. For such an adaptation, the specific characteristics of the different trace gas retrievals and the specific spatial patterns (profiles as well as global distribution) have to be considered in detail. In particular for BrO, the method will be probably insufficient, since the regions of interest for BrO are polar, i.e. solar zenith angles are high, and stratospheric BrO profiles are too low to be fully captured by the limb measurements.

The available dataset on limb longitudinal variations can be used to check and improve other stratospheric estimation algorithms, in particular advanced RS methods working with 2-D interpolation or wave fitting. This is important for current and future satellite spectrometers without the limb viewing mode. Furthermore, the information on the longitudinal dependency of stratospheric NO<sub>2</sub> CDs, as provided by SCIAMACHY limb measurements, might also be used to improve RSM stratospheric estimations for other satellite instruments, like OMI or GOME-2. However, for such applications, differences in local times of the measurements have to be considered.

*Acknowledgements.* We thank ESA and DLR for providing SCIAMACHY spectra. Sven Köhl is funded by the DFG (Deutsche Forschungsgemeinschaft). We gratefully acknowledge valuable discussions with Andreas Richter and Andreas Hilboll. We thank Folkert Boersma, Howard K. Roscoe and two anonymous reviewers for helpful comments. We are grateful to Marloes Penning de Vries for fruitful scientific discussions and editorial support.

The service charges for this open access publication have been covered by the Max Planck Society.

Edited by: F. Boersma

## References

- Beirle, S., Platt, U., Wenig, M., and Wagner, T.: Weekly cycle of NO<sub>2</sub> by GOME measurements: a signature of anthropogenic sources, *Atmos. Chem. Phys.*, 3, 2225–2232, 2003, <http://www.atmos-chem-phys.net/3/2225/2003/>.
- Beirle, S.: Estimating source strengths and lifetime of Nitrogen Oxides from satellite data, Ph.D. Thesis, University of Heidelberg, 2004.
- Boersma, K. F., Eskes, H. J., and Brinksma, E. J.: Error analysis for tropospheric NO<sub>2</sub> retrieval from space, *J. Geophys. Res.*, 109, D04311, doi:10.1029/2003JD003962, 2004.
- Boersma, K. F., Eskes, H. J., Veefkind, J. P., Brinksma, E. J., van der A, R. J., Sneep, M., van den Oord, G. H. J., Levelt, P. F., Stammes, P., Gleason, J. F., and Bucsele, E. J.: Near-real time retrieval of tropospheric NO<sub>2</sub> from OMI, *Atmos. Chem. Phys.*, 7, 2103–2118, 2007, <http://www.atmos-chem-phys.net/7/2103/2007/>.
- Bogumil, K., Orphal, J., Homann, T., Voigt, S., Spietz, P., Fleischmann, O. C., Vogel, A., Hartmann, M., Bovensmann, H., Frerick, J., and Burrows, J. P.: Measurements of molecular absorption spectra with the SCIAMACHY pre-flight model: Instrument characterization and reference data for atmospheric remote sensing in the 230–2380 nm region, *J. Photochem. Photobiol. A.*, 157, 167–184, 2003.
- Bovensmann, H., Burrows, J. P., Buchwitz, M., Frerick, J., Noël, S., Rozanov, V. V., Chance, K. V., and Goede, A. P. H.: SCIAMACHY: Mission objectives and measurement modes, *J. Atmos. Sci.*, 56(2), 127–150, 1999.
- Brühl, C. and Crutzen, P. J.: MPIC two-dimensional model, in: *The Atmospheric Effect of Stratospheric Aircraft*, 1292, edited by: Prather, M. J. and Remsberg, E. E., NASA Ref. Publications, 103–104, 1993.
- Bucsele, E. J., Celarier, E. A., Wenig, M. O., Gleason, J. F., Veefkind, J. P., Boersma, K. F., and Brinksma, E. J.: Algorithm for NO<sub>2</sub> Vertical Column Retrieval from the Ozone Monitoring Instrument, *IEEE T. Geosci. Remote*, 44(5), 1245–1258, 2006.
- Burrows, J., Weber, M., Buchwitz, M., Rozanov, V. V., Ladstädter-Weissenmayer, A., Richter, A., de Beek, R., Hoogen, R., Bramstedt, K., Eichmann, K.-U., Eisinger, M., and Perner, D.: The Global Ozone Monitoring Experiment (GOME): Mission concept and first scientific results, *J. Atmos. Sci.*, 56, 151–175, 1999.
- Butz, A., Bösch, H., Camy-Peyret, C., Chipperfield, M., Dorf, M., Dufour, G., Grunow, K., Jeseck, P., Kühl, S., Payan, S., Pepin, I., Pukite, J., Rozanov, A., von Savigny, C., Sioris, C., Wagner, T., Weidner, F., and Pfeilsticker, K.: Inter-comparison of stratospheric O<sub>3</sub> and NO<sub>2</sub> abundances retrieved from balloon borne direct sun observations and Envisat/SCIAMACHY limb measurements, *Atmos. Chem. Phys.*, 6, 1293–1314, 2006, <http://www.atmos-chem-phys.net/6/1293/2006/>.
- Deutschmann, T.: Atmospheric radiative transfer modelling using Monte Carlo methods, Diploma Thesis, Universität Heidelberg, 2009.
- Dorf, M., Bösch, H., Butz, A., Camy-Peyret, C., Chipperfield, M. P., Engel, A., Goutail, F., Grunow, K., Hendrick, F., Hrechanyy, S., Naujokat, B., Pommereau, J.-P., Van Roozendaal, M., Sioris, C., Strohm, F., Weidner, F., and Pfeilsticker, K.: Balloon-borne stratospheric BrO measurements: comparison with Envisat/SCIAMACHY BrO limb profiles, *Atmos. Chem. Phys.*, 6, 2483–2501, 2006, <http://www.atmos-chem-phys.net/6/2483/2006/>.
- Fishman, J. and Balok, A. E.: Calculation of daily tropospheric ozone residuals using TOMS and empirically improved SBUV measurements: Application to an ozone pollution episode over the eastern United States, *J. Geophys. Res.-Atmos.*, 104, 30319–30340, 1999.
- Franke, K., Richter, A., Bovensmann, H., Eyring, V., Jöckel, P., Hoor, P., and Burrows, J. P.: Ship emitted NO<sub>2</sub> in the Indian Ocean: comparison of model results with satellite data, *Atmos. Chem. Phys.*, 9, 7289–7301, 2009, <http://www.atmos-chem-phys.net/9/7289/2009/>.
- Heckel, A., Richter, A., Rozanov, A., and Burrows, J. P.: Limb Nadir Matching: Retrieval of tropospheric NO<sub>2</sub> columns using SCIAMACHY Nadir and Limb measurements, Presentation at the workshop “Tropospheric NO<sub>2</sub> measured by satellites”, 10–12 September 2007, KNMI, De Bilt, The Netherlands, online available at: [http://www.knmi.nl/research/climate\\_observations/events/no2\\_workshop/presentations/Presentations/107\\_Heckel.ppt](http://www.knmi.nl/research/climate_observations/events/no2_workshop/presentations/Presentations/107_Heckel.ppt), last access: February 2010, 2007.
- Kühl, S., Puškite, J., Deutschmann, T., Platt, U., and Wagner, T.: SCIAMACHY Limb Measurements of NO<sub>2</sub>, BrO and OClO, Retrieval of vertical profiles: Algorithm, first results, sensitivity and comparison studies, *Adv. Space Res.*, 42, 1747–1764, 2008.
- Leue, C., Wenig, M., Wagner, T., Klimm, O., Platt, U., and Jähne, B.: Quantitative analysis of NO<sub>x</sub> Emissions from Global Ozone Monitoring Experiment satellite image sequences, *J. Geophys. Res.*, 106, 5493–5505, 2001.
- Levelt, P. F., van den Oord, G. H. J., Dobber, M. R., Malkki, A., Visser, H., de Vries, J., Stammes, P., Lundell, J. O. V., and Saari, H.: The ozone monitoring instrument, *IEEE T. Geosci. Remote*, 44(5), 1093–1101, 2006.
- Martin, R. V., Chance, K., Jacob, D. J., Kurosu, T. P., Spurr, R. J. D., Bucsele, E., Gleason, J. F., Palmer, P. I., Bey, I., Fiore, A. M., Li, Q., Yantosca, R. M., and Koelemeijer, R. B. A.: An improved retrieval of tropospheric nitrogen dioxide from GOME, *J. Geophys. Res.*, 107(D20), 4437, doi:10.1029/2001JD001027, 2002.
- Martin, R. V.: Satellite remote sensing of surface air quality, *Atmos. Environ.*, 42, 7823–7843, 2008.
- Menke, W.: *Geophysical data analysis: discrete inverse theory*, Academic Press, 1999.
- Platt, U. and Stutz, J.: *Differential Optical Absorption Spectroscopy Principles and Applications*, Series: Physics of Earth and Space Environments, Springer, ISBN 978-3-540-21193-8, 2008.
- Polovina, J. J., Howell, E. A., and Abecassis, M.: Oceans least productive waters are expanding, *Geophys. Res. Lett.*, 35, L03618, doi:10.1029/2007GL031745, 2008.
- PROMOTE, PROTOCOL MOniToring for the GMES Service Element on Atmospheric Composition, online available at: <http://www.iup.uni-bremen.de/does/no2-promote.htm>, last access: February 2010, 2004.
- Puškite, J., Kühl, S., Deutschmann, T., Wilms-Grabe, W., Friedeburg, C., Platt, U., and Wagner, T.: Retrieval of stratospheric trace gases from SCIAMACHY limb measurements, Proceedings of the First Atmospheric Science Conference, 8–12 May, ESA/ESRIN, Frascati, Italy, ESA SP-628, available at: [http://earth.esa.int/workshops/atmos2006/participants/1148/paper\\_proc\\_Frasc\\_2.pdf](http://earth.esa.int/workshops/atmos2006/participants/1148/paper_proc_Frasc_2.pdf), last access: February 2010, 2006.

- Puķīte, J., Kühl, S., Deutschmann, T., Platt, U., and Wagner, T.: Accounting for the effect of horizontal gradients in limb measurements of scattered sunlight, *Atmos. Chem. Phys.*, 8, 3045–3060, 2008, <http://www.atmos-chem-phys.net/8/3045/2008/>.
- Puķīte, J., Kühl, S., Deutschmann, T., Platt, U., and Wagner, T.: Extending differential optical absorption spectroscopy for limb measurements in the UV, *Atmos. Meas. Tech. Discuss.*, 2, 2919–2982, 2009, <http://www.atmos-meas-tech-discuss.net/2/2919/2009/>.
- Puķīte, S., Kühl, T., Deutschmann, U., Platt, and Wagner, T.: Profile retrieval from SCIAMACHY limb measurements by global 2-D tomography, in preparation, 2010.
- Richter, A. and Wagner, T.: Diffuser Plate Spectral Structures and their Influence on GOME Slant column densities, Technical Note, online available at: [http://joseba.mpch-mainz.mpg.de/pdf\\_dateien/diffuser\\_gome.pdf](http://joseba.mpch-mainz.mpg.de/pdf_dateien/diffuser_gome.pdf), last access: February 2010, January 2001, 2001.
- Richter, A. and Burrows, J. P.: Tropospheric NO<sub>2</sub> from GOME Measurements, *Adv. Space Res.*, 29(11), 1673–1683, 2002.
- Richter, A., Burrows, J. P., Nüß, H., Granier, C., and Niemeier, U.: Increase in tropospheric nitrogen dioxide over China observed from space, *Nature*, 437, 129–132, doi:10.1038/nature04092, 2005.
- Sierk, B., Richter, A., Rozanov, A., von Savigny, Ch., Schmoltner, A. M., Buchwitz, M., Bovensmann, H., and Burrows, J. P.: Retrieval and monitoring of atmospheric trace gas concentrations in nadir and limb geometry using the space-borne SCIAMACHY instrument, *Environ. Monit. Assess.*, 120, 65–77, doi:10.1007/s10661-005-9049-9, 2006.
- Sioris, C. E., Kurosu, T. P., Martin, R. V., and Chance, K.: Stratospheric and tropospheric NO<sub>2</sub> observed by SCIAMACHY: first results *Adv. Space Res.*, 34(4), 780–785, 2004.
- Vandaele, A. C., Hermans, C., Simon, P. C., Carleer, M., Collins, R., Fally, S., Mérienne, M. F., Jenouvrier, A., and Coquart, B.: Measurements of the NO<sub>2</sub> absorption cross-sections from 42 000 cm<sup>-1</sup> to 10 000 cm<sup>-1</sup> (238–1000 nm) at 220 K and 294 K, *J. Quant. Spectrosc. Radiat. Transfer*, 59, 171–184, 1998.
- Vasilkov, A. P., Joiner, J., Gleason, J., and Bhartia, P.: Ocean Raman scattering in satellite backscatter UV measurements, *Geophys. Res. Lett.*, 29, 1837–1840, 2002.
- Vountas, M., Richter, A., Wittrock, F., and Burrows, J. P.: Inelastic scattering in ocean water and its impact on trace gas retrievals from satellite data, *Atmos. Chem. Phys.*, 3, 1365–1375, 2003, <http://www.atmos-chem-phys.net/3/1365/2003/>.
- Wagner, T., Beirle, S., Deutschmann, T., Eigemeier, E., Frankenberg, C., Grzegorski, M., Liu, C., Marbach, T., Platt, U., and Penning de Vries, M.: Monitoring of atmospheric trace gases, clouds, aerosols and surface properties from UV/vis/NIR satellite instruments, *J. Opt. A., Pure Appl. Opt.*, 10, 104019, doi:10.1088/1464-4258/10/10/104019, 2008.
- Wenig, M., Kühl, S., Beirle, S., Bucsel, E., Jähne, B., Platt, U., Gleason, J., and Wagner, T.: Retrieval and analysis of stratospheric NO<sub>2</sub> from the Global Ozone Monitoring Experiment, *J. Geophys. Res.*, 109, D04315, doi:10.1029/2003JD003652., 2004.
- Ziemke, J. R., Chandra, S., and Bhartia, P. K.: “Cloud slicing”: A new technique to derive upper tropospheric ozone from satellite measurements, *J. Geophys. Res.-Atmos.*, 106, 9853–9867, 2001.